Supplementary Materials

Selective electroreduction of CO_2 to C_{2+} products on cobalt decorated copper catalysts

Sanaz Soodi[1,2,3,4,#], Jun-Jun Zhang[5,6,#], Jie Zhang[1,2], Yuefeng Liu[7], Mohsen Lashgari[3,8], Spyridon Zafeiratos[9], Andreas Züttel[1,2], Kun Zhao[1,2,10,*], Wen Luo[5,*]

[1]Laboratory of Materials for Renewable Energy (LMER), Institute of Chemical Sciences and Engineering (ISIC), Basic Science Faculty (SB), École Polytechnique Fédérale de Lausanne (EPFL) Valais/Wallis, Energypolis, Sion CH-1951, Switzerland.
[2]Empa Materials Science & Technology, Dübendorf CH-8600, Switzerland.
[3]Chemistry department, Institute for Advanced Studies in Basic Sciences (IASBS), Zanjan 45137-66731, Iran.
[4]Department of Chemical and Process Engineering, University of Surrey, Guildford GU2 7XH, UK.
[5]School of Environmental and Chemical Engineering, Shanghai University, Shanghai 200444, China.
[6]Department of Chemical Engineering, Sichuan University, Chengdu 610065, Sichuan, China.
[7]Dalian National Laboratory for Clean Energy (DNL), Dalian Institute of Chemical Physics (DICP), Chinese Academy of Science, Dalian 116023, Liaoning, China.
[8]Center for Research in Climate Change and Global Warming: Hydrogen and Solar Division, Zanjan 45137-66731, Iran.
[9]Institute for Chemistry and Energy, Environment and Health processes (ICPEES) - UMR 7515 CNRS - University of Strasbourg, Strasbourg 67087, France.
[10]Department of Chemistry, University of Washington, Seattle, WA 98195-1700, USA.
[#]Authors contributed equally.

[*]**Correspondence to:** Dr. Kun Zhao, Laboratory of Materials for Renewable Energy (LMER), Institute of Chemical Sciences and Engineering (ISIC), Basic Science Faculty (SB), École Polytechnique Fédérale de Lausanne (EPFL) Valais/Wallis, Energypolis, Rue de I'Industrie 17, Sion CH-1951, Switzerland. Email: kzhao20@uw.edu; Prof. Wen Luo, School of Environmental and Chemical Engineering, Shanghai University, 99 Shangda Road, Shanghai 200444, China. E-mail: wenluo@shu.edu.cn

1. Experimental details

1.1 Materials

$KHCO_3$ (≥99.8 %), $Co(NO_3)_2.6H_2O$ (≥99.8 %), NaOH (≥99.8 %), $(NH_4)_2S_2O_8$ (≥99.8 %) and HNO_3 (%) were purchased from Sigma Aldrich. Cu foils of 0.125 mm thicknesses (99.9% purity) were purchased from Good fellow, U.K. An Ag/AgCl reference electrode (3 M NaCl) was purchased from ALS Corporation, Japan. High-purity CO_2 (99.999%) and N_2 (99.999%) were from Cabagas, Switzerland. All chemicals were used as purchased without further purification.

1.2 Preparation of the Cu NWs sample

$Cu(OH)_2$ NWs were prepared using a chemical oxidation method following our previous work.[1] First, Cu foil was cut to a flag shape with an active size of 1 × 0.5 cm^2. To remove the surface copper oxides and other impurities, the Cu foil was cleaned via sonication in acetone, water and diluted HNO_3 solution, respectively. Next, the Cu foil was rinsed with Milli-Q water and dried under N_2 flow. The clean Cu foil was immersed in a mixed solution of 2.5 M NaOH and 0.125 M $(NH_4)_2S_2O_8$ for 10 min to grow $Cu(OH)_2$ NWs. Finally, the Cu foil with a layer of $Cu(OH)_2$ NWs was rinsed with Milli-Q water and dried under the N_2 flow.

1.3 Preparation of the $CuCo_x$ catalysts

Co was deposited on $Cu(OH)_2$ NWs by a facile dip coating method.[1] To control the loading of Co, a serious of $Co(NO_3)_2$ solutions of various concentrations (2, 5, 10, 20, and 50 mM) were prepared with Milli-Q water. Then the as-prepared Cu foil with $Cu(OH)_2$ NWs was dipped into a $Co(NO_3)_2$ solution for 30 s to adsorb $Co(NO_3)_2$. After that, the sample was dried with N_2 and annealed in air at 150 °C for 2 h to get the CoO_x/CuO precursor. During CO_2RR, the final reduced $CuCo_x$ samples can be obtained. The x values of 0.07 at. %, 0.2 at. %, 0.4 at. %, 1.1 at. %, and 1.8 at. % correspond to the $Co(NO_3)_2$ solution of 2, 5, 10, 20, and 50 mM, respectively.

1.4 Characterization

The X-ray diffraction (XRD) patterns of the samples were obtained by using X-ray diffraction (XRD) patterns were obtained from a Bruker D8 Discovery (Germany) equipped with a Cu Kα X-ray source at 40 kV and 40 mA. The X-ray photoelectron spectroscopy (XPS) was performed with a Kratos Axis Supra system, using a monochromated Al Kα (1486.6 eV) X-ray source at a nominal power of 225W. No charge compensation was required, and the binding energies (BEs) were referenced to

C 1s at 284.5 eV. A pass energy of 20 eV was used for acquiring all core level and Auger electron spectra. Scanning electron microscopy (SEM) images were collected on a FEI Teneo system. Transmission electron microscopy (TEM) and energy dispersive X-ray (EDX) analyses were performed on a FEI Tecnai Osiris at an acceleration voltage of 200 kV. This microscope is equipped with a high brightness X-FEG gun and silicon drift Super-X EDX detectors. High-angle annular dark-field (HAADF) images and EDX elemental maps were acquired in scanning TEM (STEM) mode. The chemical composition of the catalyst was analyzed using the inductively coupled plasma optical emission spectrometry system (ICP-OES, Agilent 5110).

1.5 Electrochemical Reduction of CO_2

Electrochemical reduction of CO_2 on the Cu NWs and $CuCo_x$ samples were carried out in an H-type electrochemical cell, and the Autolab PGSTAT302N potentiostat was used for electrochemical analysis. The compartments of the cell were separated by a Nafion membrane. A Platinum wire and Ag/AgCl (3 M NaCl) electrode were applied as the counter and reference electrodes, respectively. CO_2 was continuously infused into cathode compartments at a rate of 20 mL/min (EL-Flow, Bronkhorst) during the experiment. The applied potentials were recorded against the Ag/AgCl (3 M NaCl) reference electrode and compensated for iR loss and converted versus the reversible hydrogen electrode (RHE): E(V vs RHE) = E(V vs Ag/AgCl) + 0.197V + (0.0591 × pH).

1.6 Product Analysis

Gaseous products including H_2, CO and C_2H_4 were quantified with a gas chromatography (GC SRI instruments 8610C) equipped with TCD and FID detectors. At the end of electrolysis, liquid products were collected and quantified with NMR (Bruker 400 mHz). Faradaic efficiency for every sample was obtained following the equations: $nF = \frac{nFC_i\nu P}{jRT}$ and $nF = \frac{nFC_iV}{Q}$ for gas and liquid product, respectively. n is the number of electrons transferred to produce one molecule of the target product i, F is the faradaic efficiency, C_i is the concentration of the target product i which is determined by GC or NMR, ν is the flow rate of CO_2 bubbled in to the electrolyte, P and T are the pressure (101 325 Pa) and temperature (22 °C) of the gas sampled by the GC sample loop, respectively, j is the total current when sampling, R is the gas constant, V is the volume of the electrolyte, and Q is the total charge transfer to produce the target product.

1.7 In situ Raman spectroscopy test

In situ Raman spectroscopy was performed using a home-built Raman cell. The incident and scattered beams were sent to the sample and collected through an immersion objective, respectively (Leica, 63×). A laser beam with a wavelength of 632 nm was used. 0.1M $KHCO_3$ was used as the electrolyte, and CO_2 was continuously passed into the electrolyte.

1.8 In situ infrared spectroscopy test

ATR-SERAS measurements were made on a Nicolet iS10 FTIR spectrometer equipped with an MCT-A detector at an incidence Angle of approximately 50°. Infrared spectra were obtained with a spectral resolution of 4 cm^{-1}. All spectra are expressed in absorbance. To prepare the electrode, a catalyst ink was dropped onto a silicon crystal deposited with an Au film and assembled into a self-assembled spectroelectrochemical cell for ATR-SERAS measurement. The Autolab PGSTAT302N electrochemical workstation was used for potential control and current measurement during the test. Before each spectrum collection, the optical path was degassed with high purity N_2 to eliminate interference of H_2O and CO_2 in the air. During the test, CO_2 gas was continuously injected into 0.1M $KHCO_3$ solution.

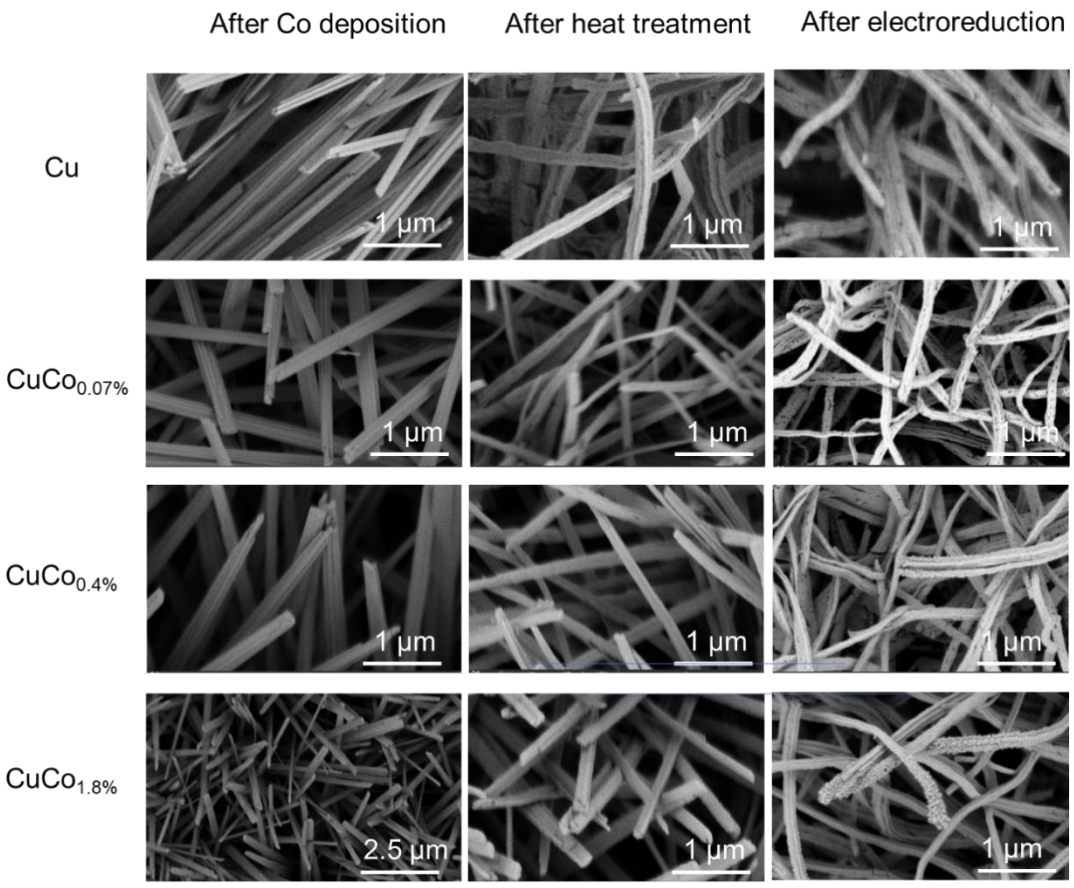

Supplementary Figure 1. SEM images of Cu, $CuCo_{0.07\%}$, $CuCo_{0.4\%}$, and $CuCo_{1.8\%}$ samples after different treatments: after Co deposition (except for the pure Cu sample), after heat treatment, and after electroreduction.

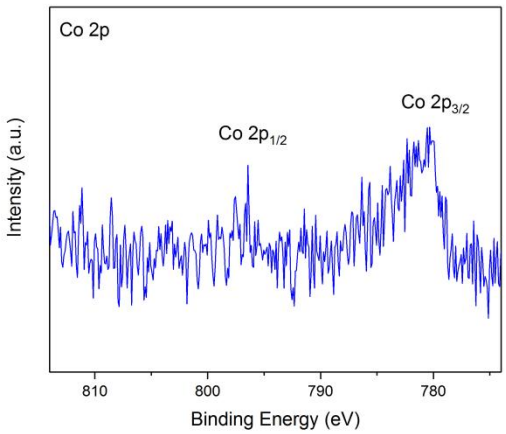

Supplementary Figure 2. Co 2p XPS spectrum of the $CuCo_{0.4\%}$ sample.

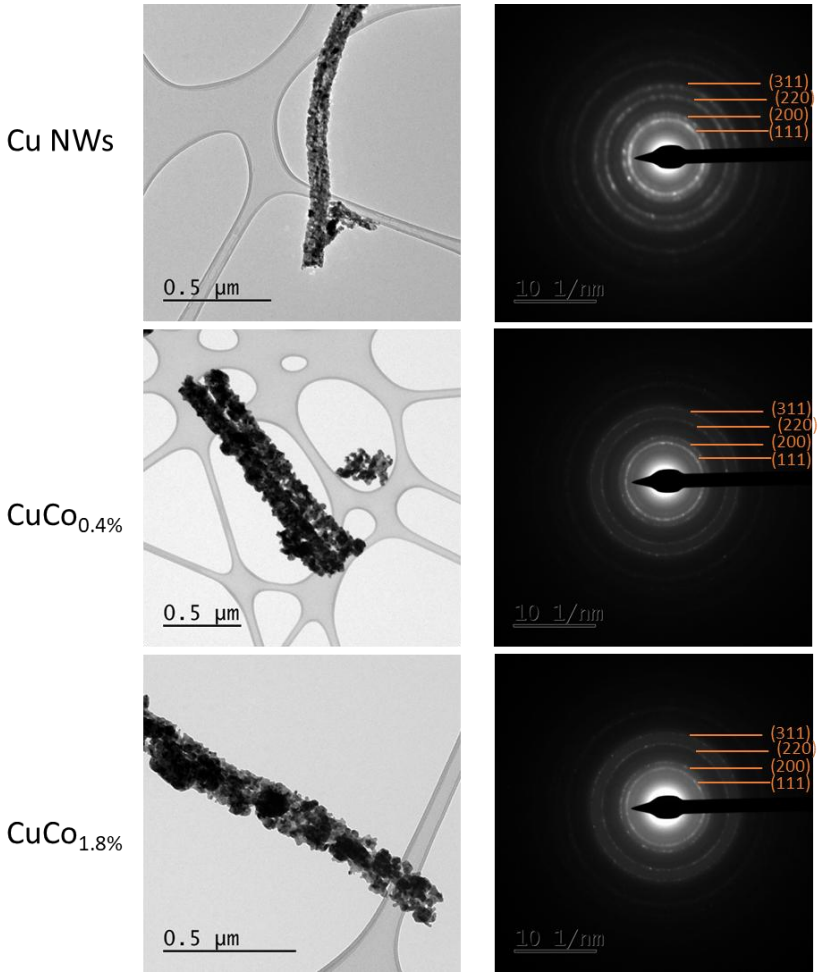

Supplementary Figure 3. TEM images and the corresponding SAED patterns of Cu and $CuCo_x$ samples. The diffraction rings indicated in the SAED patterns are from metallic Cu.

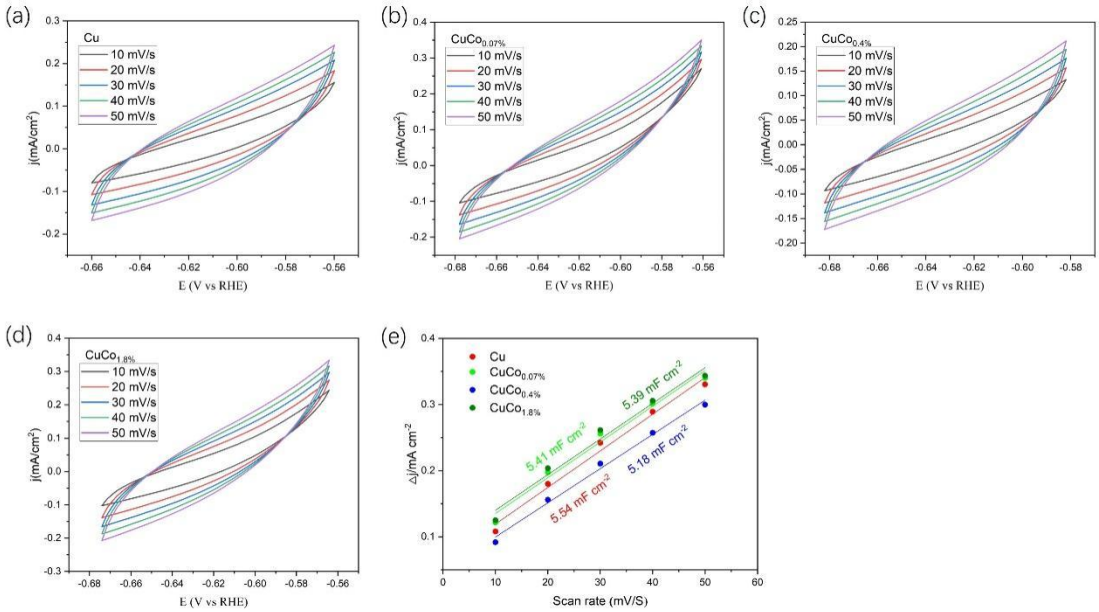

Supplementary Figure 4. CV curves for (a) Cu, (b) $CuCo_{0.07\%}$, (c) $CuCo_{0.4\%}$, and (d) $CuCo_{1.8\%}$. (e) C_{dl} values of Cu, $CuCo_{0.07\%}$, $CuCo_{0.4\%}$, and $CuCo_{1.8\%}$ obtained by plotting Δj *vs*. scan rate.

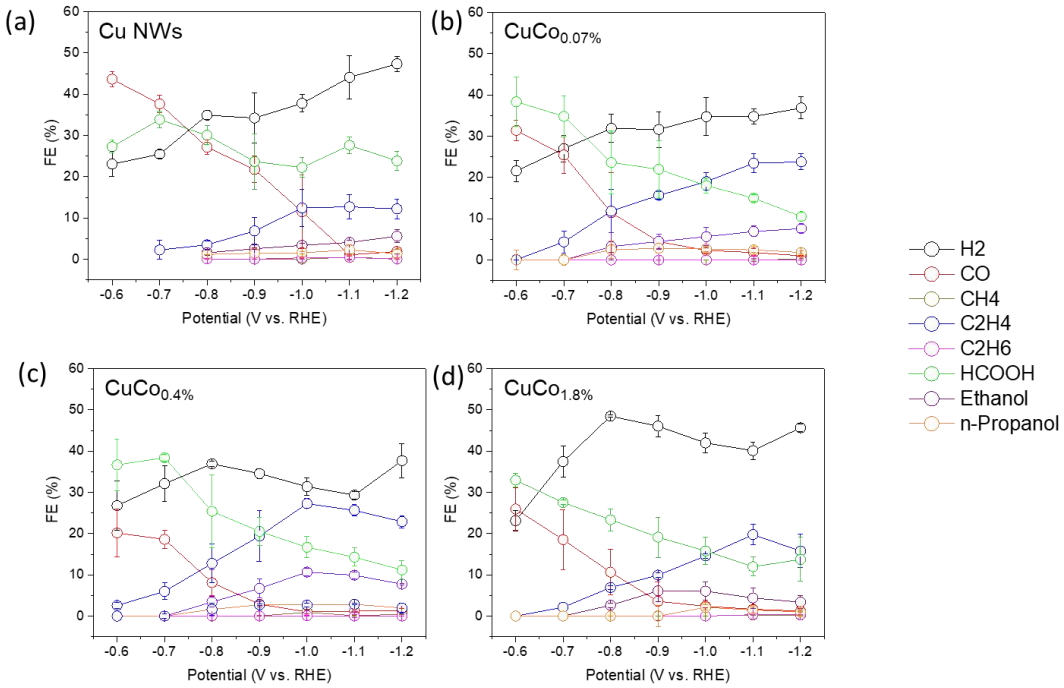

Supplementary Figure 5. Faradaic efficiencies for (a) Cu NWs, (b) $CuCo_{0.07\%}$, (c) $CuCo_{0.4\%}$, and (d) $CuCo_{1.8\%}$.

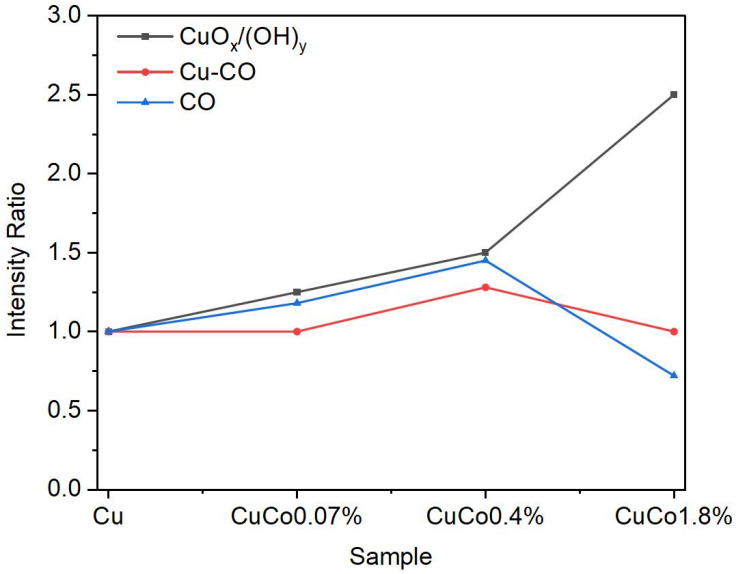

Supplementary Figure 6. Raman peaks ratios for Cu, $CuCo_{0.07\%}$, $CuCo_{0.4\%}$, and $CuCo_{1.8\%}$ samples. The intensity ratios were obtained by dividing the peak intensity of $CuCo_x$ sample by the corresponding peak intensity of the Cu sample. The *Cu oxide* represents the peak at 490 cm^{-1}, *Cu-CO* represents the accumulation of peaks at 280 and 360 cm^{-1}, and *CO* represents the peak at ~2090 cm^{-1}.

Supplementary Table 1. Comparison of CO_2RR performance of various CuCo catalysts

Catalysts	Electrolyte	Potential （vs. RHE）	C_{2+} Current density （mA cm^{-2}）	C_{2+} FE （%）	Refs
$CuCo_{0.4\%}$	0.10 M $KHCO_3$	-1.0	9	40.7	This Work
Co-doped CuO	1.0 M $KHCO_3$	-1.07	108	15.56	[1]
$CuNWs_{10}$-CoPc	1.0 M KOH	-1.4	-	42.9	[2]
Cu-Co NPs	0.5 M [Bmim]PF_6/MeCN	-1.5	~ 2	< 3	[3]
$CuCo_3$	0.50 M $KHCO_3$	-1.5	~ 30	~ 30	[4]
$Cu_{50}Co_{50}$	0.10 M $KHCO_3$	-1.1	~ 0	~ 0	[5]
CoCu-DASC	0.50 M $KHCO_3$	-1.0	< 1.5	< 10	[6]

REFERENCES

[1] B. Kim, Y.C. Tan, Y. Ryu, K. Jang, H.G. Abbas, T. Kang, H. Choi, K.-S. Lee, S. Park, W. Kim, P.-P. Choi, S. Ringe, J. Oh, Trace-Level Cobalt Dopants Enhance CO_2 Electroreduction and Ethylene Formation on Copper, ACS Energy Letters, 8 (2023) 3356-3364.

[2] Y. Luo, J. Yang, J. Qin, K. Miao, D. Xiang, A. Kuchkaev, D. Yakhvarov, C. Hu, X. Kang, Cobalt phthalocyanine promoted copper catalysts toward enhanced electro reduction of CO_2 to C_2: Synergistic catalysis or tandem catalysis?, Journal of Energy Chemistry, 92 (2024) 499-507.

[3] W. Guo, J. Bi, Q. Zhu, J. Ma, G. Yang, H. Wu, X. Sun, B. Han, Highly Selective CO2 Electroreduction to CO on Cu–Co Bimetallic Catalysts, ACS Sustainable Chemistry & Engineering, 8 (2020) 12561-12567.

[4] Y. Yan, Z. Zhao, J. Zhao, W. Tang, W. Huang, J.-M. Lee, Atomic-thin hexagonal CuCo nanocrystals with d-band tuning for CO_2 reduction, Journal of Materials Chemistry A, 9 (2021) 7496-7502.

[5] M. Bernal, A. Bagger, F. Scholten, I. Sinev, A. Bergmann, M. Ahmadi, J. Rossmeisl, B.R. Cuenya, CO2 electroreduction on copper-cobalt nanoparticles: Size and composition effect, Nano Energy, 53 (2018) 27-36.

[6] J.d. Yi, X. Gao, H. Zhou, W. Chen, Y. Wu, Design of Co-Cu Diatomic Site Catalysts for High-efficiency Synergistic CO2 Electroreduction at Industrial-level Current Density, Angewandte Chemie International Edition, 61 (2022) e202212329.